metals

Article

Homogenisation Efficiency Assessed with Microstructure Analysis and Hardness Measurements in the EN AW 2011 Aluminium Alloy

Maja Vončina [1,*], Aleš Nagode [1], Jožef Medved [1], Irena Paulin [2], Borut Žužek [2] and Tilen Balaško [1]

[1] Department for Materials and Metallurgy, Faculty of Natural Sciences and Engineering, University of Ljubljana, Aškerčeva 12, 1000 Ljubljana, Slovenia; ales.nagode@omm.ntf.uni-lj.si (A.N.); jozef.medved@omm.ntf.uni-lj.si (J.M.); tilen.balasko@omm.ntf.uni-lj.si (T.B.)

[2] Institute of Metals and Technology, Lepi Pot 11, 1000 Ljubljana, Slovenia; irena.paulin@imt.si (I.P.); borut.zuzek@imt.si (B.Ž.)

* Correspondence: maja.voncina@omm.ntf.uni-lj.si

Abstract: When extruding the casted rods from EN AW 2011 aluminium alloys, not only their homogenized structure, but also their extrudable properties were significantly influenced by the hardness of the alloy. In this study, the object of investigations was the EN AW 2011 aluminium alloy, and the effect of homogenisation time on hardness was investigated. First, homogenisation was carried out at 520 °C for different times, imitating industrial conditions. After homogenisation, the samples were analysed by hardness measurements and further characterised by microscopy and image analysis to verify the influence of homogenisation on the resulting microstructural constituents. In addition, non-equilibrium solidification was simulated using the program Thermo-Calc and phase formation during solidification was investigated. The homogenisation process enabled more rounded shape of the Al_2Cu eutectic phase, equilibrium formation of the phases, and the precipitation in the matrix, leading to a significant increase in the hardness of the EN AW 2011 aluminium alloy. The experimental data revealed a suitable homogenisation time of 4–6 h at a temperature of 520 °C, enabling optimal extrusion properties.

Keywords: EN AW 2011 aluminium alloy; thermodynamic equilibrium; intermetallic phases; eutectic; homogenisation; hardness

check for updates

Citation: Vončina, M.; Nagode, A.; Medved, J.; Paulin, I.; Žužek, B.; Balaško, T. Homogenisation Efficiency Assessed with Microstructure Analysis and Hardness Measurements in the EN AW 2011 Aluminium Alloy. *Metals* **2021**, *11*, 1211. https://doi.org/10.3390/met11081211

Academic Editor: JaeHwang Kim

Received: 5 July 2021
Accepted: 27 July 2021
Published: 29 July 2021

1. Introduction

Al-Cu based 2xxx alloys offer high strength with low specific weight and are widely used in the form of extrusions for major structural components, particularly in the aircraft industry. However, these alloys exhibit low extrusion rates, require high extrusion pressure, and are therefore assigned a low extrudability index [1,2]. As ingots are cast, non-equilibrium solidification usually results in micro-sized eutectic phases with a relatively low melting point [3–5] that are likely to melt and cause irreversible damage during thermomechanical treatments at high temperatures [6]. The low-temperature annealing is less effective in eliminating eutectics and micro-segregation of dissolved elements due to insufficient solid solubility and limited diffusivity of alloying elements. Consequences of non-equilibrium solidification also include crystal segregation, unfavourable shape of intermetallic phases, and inhomogeneous distribution of alloying elements in the rods or ingots and throughout the microstructure [7–9].

Homogenisation prior to extrusion must be adequate to achieve a suitable homogenised microstructure and optimum hardness of the cast rods. Cast ingots must undergo a homogenisation treatment before extrusion to eliminate micro-segregation, modify the intermetallic phase type, and morphology to improve extrudability [6,10]. It is evident that microstructural changes such as transformation of large constituent particles, formation of dispersoids, and precipitation/dissolution of precipitates during homogenisation affect the subsequent extrusion behaviour and microstructural evolution. The development of the microstructure and the effect on the final properties are influenced by both alloy additions and heat treatment parameters [11,12]. In addition, precipitation is also controlled in this way [4].

These large residual and non-equilibrium constituents, such as the θ-Al_2Cu phase in aluminium alloys of the 2xxx series, are highly enriched in solute atoms, causing a considerable dissolving effort that affects the corresponding strengthening behaviour and increases the cost [13,14]. For instance, the main purpose of introducing silicon as an alloying element in the multicomponent EN AW 2014 aluminium alloy was to improve the strength and welding properties [15,16]. In addition, it has been widely reported that adding traces of silicon to the Al-Cu-Mg alloy can significantly accelerate the age-hardening response and improve the peak hardness due to the induction of heterogeneous nucleation [17,18]. The microstructure of the EN AW 2011 aluminium alloy consists of primary α-Al crystals, a needle-shaped $Al_9Fe_2Si_2$ eutectic phase occurring at the crystal grain boundaries, an Al_2Cu eutectic phase, and solid roundish particles of lead and bismuth [9,18,19]. Rods are mainly produced by direct chill casting (DC) and may have different manganese and iron contents [20].

The homogenisation process also serves as a solution treatment required for the subsequent age hardening process. During the homogenisation process, the secondary phases are dissolved in two stages, which together control the dissolution kinetics (atom transfer across the particle-matrix interface and solute diffusion away from the interface) [20]. Another factor that affects the dissolution kinetics is how far the system is from the equilibrium (homogenised) state, which gives the system the driving force towards the equilibrium state. This factor is dictated by the casting process [7].

To ensure proper homogenisation prior extrusion, this study investigated the appropriate homogenisation time to achieve a suitable homogenised microstructure and optimum hardness and consequently extrudability via hardness measurements and microstructure analysis.

2. Materials and Methods

The influence of the homogenisation process on the hardness and microstructural homogeneity was studied for the EN AW 2011 aluminium alloy (European Standard EN 573-3, Table 1), partially changing the chemical composition. According to the standard, lead was replaced by bismuth and silicon in the studied alloy, since lead is a heavy and toxic metal. The prediction of phase formation in a certain temperature range (homogenisation temperature), which significantly affects the mechanical and forming properties of the alloy, was calculated. From the actual chemical composition obtained by ICP analysis (inductively coupled plasma optical emission spectrometry (ICP-OES, Agilent 720, Mulgrave, Australia), calculations were performed using the computer software Thermo-Calc 2020a (accessed on 15 March 2021) and the TCAL6 database (Thermo-Calc Software AB, Stockholm, Sweden).

Table 1. Chemical composition of the EN AW 2011 aluminium alloy/wt.% [21].

Element	Cu	Bi	Fe	Pb	Si	Al
Concentration	5.0–6.0	0.20–0.60	up to 0.70	0.20–0.60	up to 0.40	Rest

The effect of homogenisation annealing on hardness, which determines extrusion properties, was assessed by various analysis. First, as-cast samples from a rod were prepared in the form of a cube with dimensions 15 mm × 15 mm × 15 mm and homogenised in a calibrated and precisely controlled electric chamber furnace, imitating industrial homogenisation conditions. Samples were placed in the furnace as it was heated at the testing temperature and cooled in air after certain homogenisation times. Homogenisation annealing was carried out at 520 °C and lasted for 4, 5, 6, 7, 8, 9, 10, 11, and 12 h, with the as-cast sample as the initial condition.

For hardness measurements and microstructure analysis, specimens after homogenisation were cast in cold epoxy and prepared metallographically according to the standard metallographic procedure for aluminium alloys. Polishing was based on MDNAP 300 mm to which a diamond suspension was added. The final polishing was based on MDChem using the suspension OPS.

Hardness of investigated alloy was determined according to SIST EN ISO 6506-1:2014 using INNOVATEST NEXUS 7500 (NEXUS 7500, Maastricht, The Netherlands) where HBW 2.5/62.5 was measured. Beside this Vickers hardness (HV0.05) using Instron Tukon 2100B (Wilson Instruments, Norwood, MA, USA) according to SIST EN ISO 6507-1:2018 was also measured. The combination of two different hardness measurement techniques enabled us to investigate macro hardness (HBW) of the investigated alloy indicating extrusion index, as well as micro hardness (HV) where hardening of the matrix of aluminium alloy was measured after different homogenisation times.

The samples for differential scanning calorimetry analysis (DSC) and homogenisation simulation on the DSC instrument (a STA Jupiter 449c instrument (NETZSCH Group, Selb, Germany)), were prepared in the form of a cylinder with 5 mm diameter and 3 mm height. DSC analysis was performed as follows: heating up to 720 °C and cooled to a room temperature using a heating/cooling rate of 10 K/min in a protective atmosphere of argon. From the DSC curves the solidus temperature and solidification characteristic temperatures were determined in order to verify calculated equilibrium results from the software Thermo-Calc. Homogenisation of the as-cast samples on the DSC instrument was set for 12 h at 520 °C, whereas the heating/cooling rate were set at 20 K/min and argon protective atmosphere was used. The tangent method was used to determine the change in the slope of the DSC curves, which was also attributed to changes during homogenisation.

Scanning electron microscopy (SEM) and energy dispersion X-ray spectroscopy (EDS) were used to perform phase analysis after different homogenisation annealing times using a Thermo Fisher Scientific Quattro S FEG-SEM microscope (Thermo Fisher Scientific, Waltham, MA, USA) with an Oxford Ultim Max SDD EDS analyser (Oxford Instruments, Abingdon, UK). EDS elemental mapping and EDS microstructure constituents in the as-cast state and after specific homogenisation times were prepared.

3. Results and Discussion

Figure 1a shows the calculated amount of all phase equilibria with respect to temperature of an EN AW 2011 aluminium alloy using TCAL6 database, calculated per 100 g of alloy. The results show that the temperature range for the dissolution is 450–540 °C. This diagram implies that when heated to 520 °C for a long holding time, Al_2Cu and a portion of Al_7Cu_2Fe dissolve, $Al_{15}Si_2Mn_4$ and $Al_9Fe_2Si_2$ completely dissolve, while the iron phase $Al_{13}Fe_4$, as well as portion of Al_7Cu_2Fe, is still present. The dissolution of Al_7Cu_2Fe starts according to the Thermo-Calc predicted phase stability at 390 °C and Al_2Cu at 500 °C, which corresponds to the experimental results reported in some studies [22]. The results are presented below. According to the shown calculated diagram, the homogenisation treatment for this alloy should not be carried out at temperatures above 540 °C, as the alloy will start to melt. Focusing on the solubility of the elements in the matrix (Figure 1b), which significantly affect the hardness of the matrix, the solubility of copper and silicon in the α-Al increases and almost reaches the maximum value at a temperature of 520 °C.

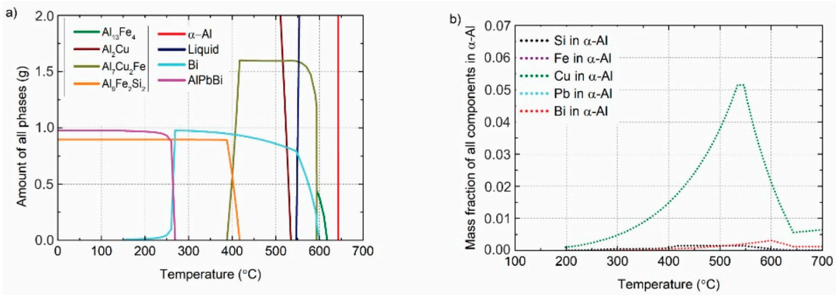

Figure 1. Thermo-Calc predicted phase stability (**a**) and element solubility in α-Al matrix (**b**) in aluminium alloy EN AW 2011 with respect to temperature.

Results from DSC analysis are presented in Figure 2 indicating solidus temperature at 541.5 °C in heating DSC curve (blue). At this temperature, the incipient melting will occur as Cu-based eutectic starts to melt. At further heating also Fe-based eutectic and α-Al matrix starts to melt, respectively. The solidification is taking place in reverse order. These results confirm homogenisation temperature predicted by software Thermo-Calc, which is supposed to be 20 °C below the nonequilibrium solidus temperature of the alloy.

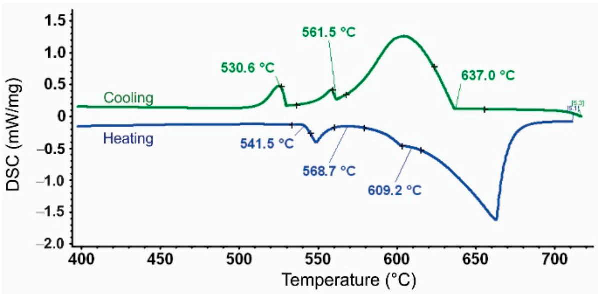

Figure 2. Results from DSC analysis of as-cast sample from EN AW 2011 aluminium alloy.

The result of simulation of homogenisation performed by DSC measurement, is shown in Figure 3. The results show that when the EN AW 2011 aluminium alloy is homogenised at 520 °C, most of the homogenisation process is completed after 4 h (marked with black arrow). To confirm the suitability of the homogenisation conditions according to the DSC measurement, the hardness results are also shown in the same figure. According to these results, the alloy reaches a hardness of 88 HBW after 4 h, presenting by more than 40% increase in hardness compared to the as-cast state (being only 63 HBW). This is quite a significant increase in hardness, which allows the alloy to still have good extrudability [23,24]. Further homogenisation time causes a further increase in hardness, making the alloys less extrudable. Another factor affects the subsequent extrusion behaviour, namely the solubility of all alloying elements in the matrix. For this reason, Vickers hardness measurements were performed in the α-Al matrix. In this case, after 4 h of homogenisation, the hardness increases by over 100% compared to the as-cast condition and continues to increase, which also accounts for the downstream of extrusion behaviour.

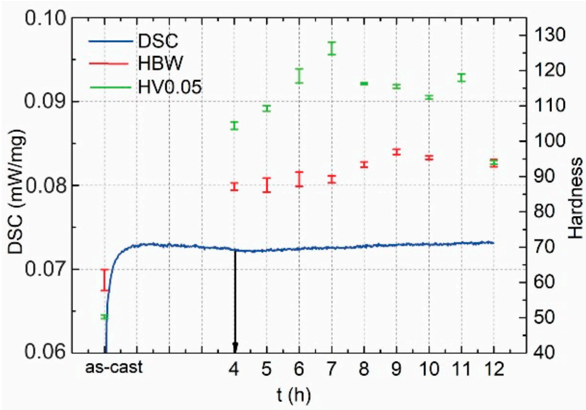

Figure 3. DSC measurement of homogenisation annealing of EN AW 2011 aluminium alloy at 520 °C 12 h and hardness results of alloy (HBW) and matrix (HV).

SEM micrographs (Figure 4) of all present microstructural constituents were made in order to analyse the influence of homogenisation time on elemental composition. All samples were analysed, but only a few are shown in Figure 4. It seems that the diffusion of elements at higher temperatures is accelerated and goes to an equilibrium state. According to the EDS analysis of this phase, the ratio of Al:Cu approaches 2:1 with longer homogenisation time (Figure 4e), containing also a small amount of iron and silicon, which appear as a consequence of element solubility in analysed phase or analysis error (analysis in depth). The eutectic Al_2Cu phase appears to be more compact as one approaches equilibrium conditions. Considering the matrix, the concentration of copper in the matrix also increases (Figure 5a, EDS results) due to a diffusion factor that also allows the precipitation of particles within the matrix (Figure 5b). EDS results showed no other elements in the matrix. The existence of precipitates in this investigated alloy was confirmed as the as-cast sample was heated to the precipitation area (310 °C) where the precipitation intensity is the greatest and various transition precipitates (θ′ and θ″, marked with red arrows). Additionally, some equilibrium θ precipitates (marked with black arrows) were formed (Figure 5b) and as the as-cast sample was heated to temperature of homogenisation 520 °C where the equilibrium precipitates θ (marked with black arrows) were established (Figure 5c) [25]. According to these results, it can be assumed that up to approximate 6.5 h of homogenisation time, hardening Cu-based phases are formed, which provide the maximum hardness of copper containing alloys, while for longer homogenisation times, a decrease in hardness is observed due to equilibrium θ precipitates [26]. This is the reason for such an extreme increase in hardness of the α-Al matrix with homogenisation time.

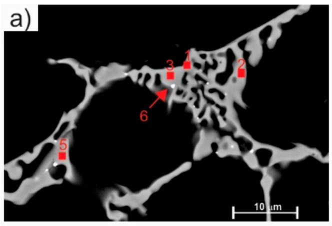

Spectrum Label / Element	1	2	3	5	6	Matrix
Al	72.9	70.2	77.5	77.1	66.7	98.8
Si	0.4	0.6	0.6	0.6	0.6	
Fe	6.5	0.1	0.1	0.1	2.8	
Cu	20.2	29.1	21.8	22.3	9.4	1.2
Bi					20.6	
Predicted phase	$Al_{13}Fe_4$	Al_2Cu	Al_2Cu	Al_2Cu	Bi-particle	α-Al

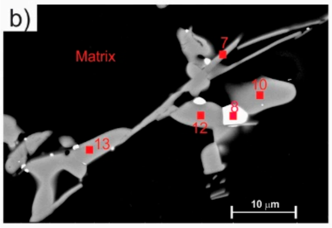

Spectrum Label / Element	7	8	10	12	13	Matrix
Al	82.4	10.9	85.0	69.1	72.4	95.2
Si	0.2	0.5	0.2	0.2	0.2	
Fe	4.3	0.50			0.1	
Cu	13.1	8.0	14.8	30.7	27.3	4.8
Bi		80.1				
Predicted phase	Al_7Cu_2Fe	Bi-particle		Al_2Cu	Al_2Cu	α-Al

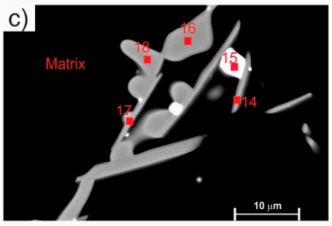

Spectrum Label / Element	14	15	16	17	18	Matrix
Al	84.7	10.9	70.4	82.5	72.0	95.1
Si	0.2					
Fe	3.7	0.5		3.9		
Cu	11.4	6.4	29.6	13.7	28.0	4.9
Bi		82.2				
Predicted phase	Al_7Cu_2Fe	Bi-particle	Al_2Cu	Al_7Cu_2Fe	Al_2Cu	

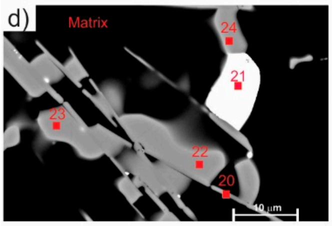

Spectrum Label / Element	20	21	22	23	24	Matrix
Al	87.7	6.9	68.5	71.3	73.3	95.2
Si	0.1		0.2	0.3	0.2	
Fe	3.1		0.1	0.1	0.1	
Cu	9.1	6.0	31.2	28.4	26.4	4.8
Bi		87.2				
Predicted phase	Al_7Cu_2Fe	Bi-particle	Al_2Cu	Al_2Cu	Al_2Cu	α-Al

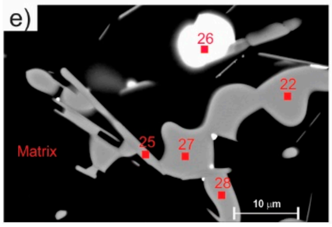

Spectrum Label / Element	25	26	27	28	29	Matrix
Al	78.6	5.6	68.8	68.6	70.4	94.0
Si			0.3	0.3	0.2	
Fe	5.6		0.1			
Cu	15.8	5.4	30.8	31.2	29.4	6.0
Bi		89.2				
Predicted phase	Al_7Cu_2Fe	Bi-particle	Al_2Cu	Al_2Cu	Al_2Cu	α-Al

Figure 4. SEM micrographs of microstructural constituents of the sample in as-cast state (**a**) and after 4 (**b**), 5 (**c**), 6 (**d**), and 12 (**e**) h of homogenisation at 520 °C, with the corresponding EDS results shown in at. %.

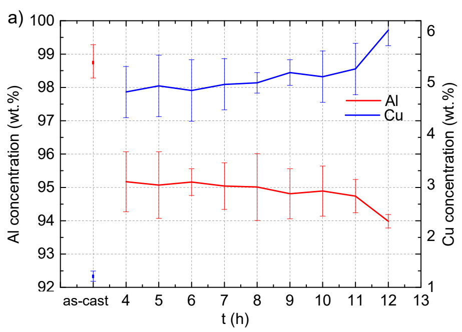

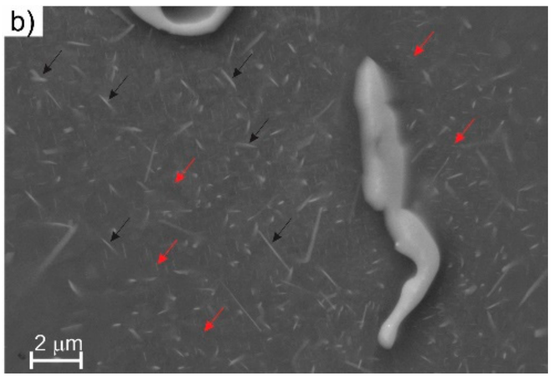

Figure 5. *Cont.*

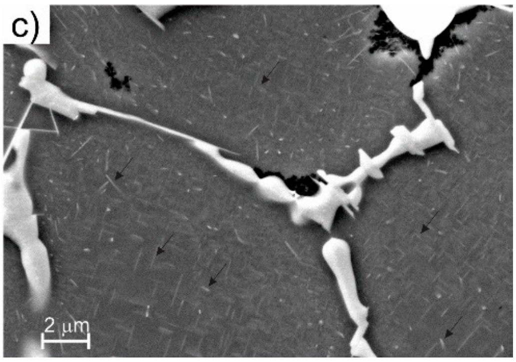

Figure 5. Content of Al and Cu in the α-Al matrix from EDS analysis as a function of homogenisation time analyzed with EDS (**a**) and SEM image of particles/precipitates formed after homogenisation annealing at 310 °C (**b**) and 520 °C (**c**) in the investigated EN AW 2011 aluminium alloy. Black arrows are marking equilibrium θ precipitates and red arrows are marking transition precipitates θ′ and θ″.

To verify previous findings, EDS individual elemental maps of as-cast and homogenised specimens at 520 °C for 4, 5, 6, 7, and 12 h from the EN AW 2011 aluminium alloy were performed and are shown in Figure 6a–f. In the as-cast sample, there is at most a finely distributed Al_2Cu eutectic containing traces of silicon, which occurs in longer $Al_{13}Fe_4$ needles. The distribution of the phase along the grain boundary becomes discontinuous due to partial dissolution of Al_2Cu eutectic and increased solubility of copper in α-Al. Comparing the microstructure in the as-cast and homogenised states, the eutectics form a continuous network in the as-cast state, which is partially broken by homogenisation. The EDS analysis shows that the Al_2Cu partially dissolved into the matrix. The result shows that the non-equilibrium eutectic phase is gradually dissolved into the matrix as the time of homogenisation increases, which is a consequence of a tendency to reach an equilibrium state.

In addition, the Al_2Cu eutectic phase forms a more rounded and compact shape upon homogenisation. This is since Cu-phase did not solidify in equilibrium in the as-cast state and is partially dissolving by heat treatment, starting at the boundary Al_2Cu eutectic phase-α-Al, reaching energetically more favorable (lower) phase boundary conditions. When the holding time is further extended, there is no obvious further dissolution of the phase. With longer homogenisation time, the $Al_{13}Fe_4$ needles become slightly larger and rounder due to energetically more favorable phase boundary conditions, which is desirable because of their lower cuttability and thus better mechanical and forming properties. Bi particles are also present in the microstructure of the EN AW 2011 aluminium alloy in all cases, whereas they appear larger with holding homogenisation time due to a high temperature diffusivity and assembling one with another (Figure 6). The most obvious effect of homogenisation can be observed after 4 h, but at a later time this effect does not change so clearly. On closer inspection, the blue colour in the Al_2Cu eutectic phase becomes more intense with longer homogenisation time, indicating a higher concentration of copper in this microstructure constituent.

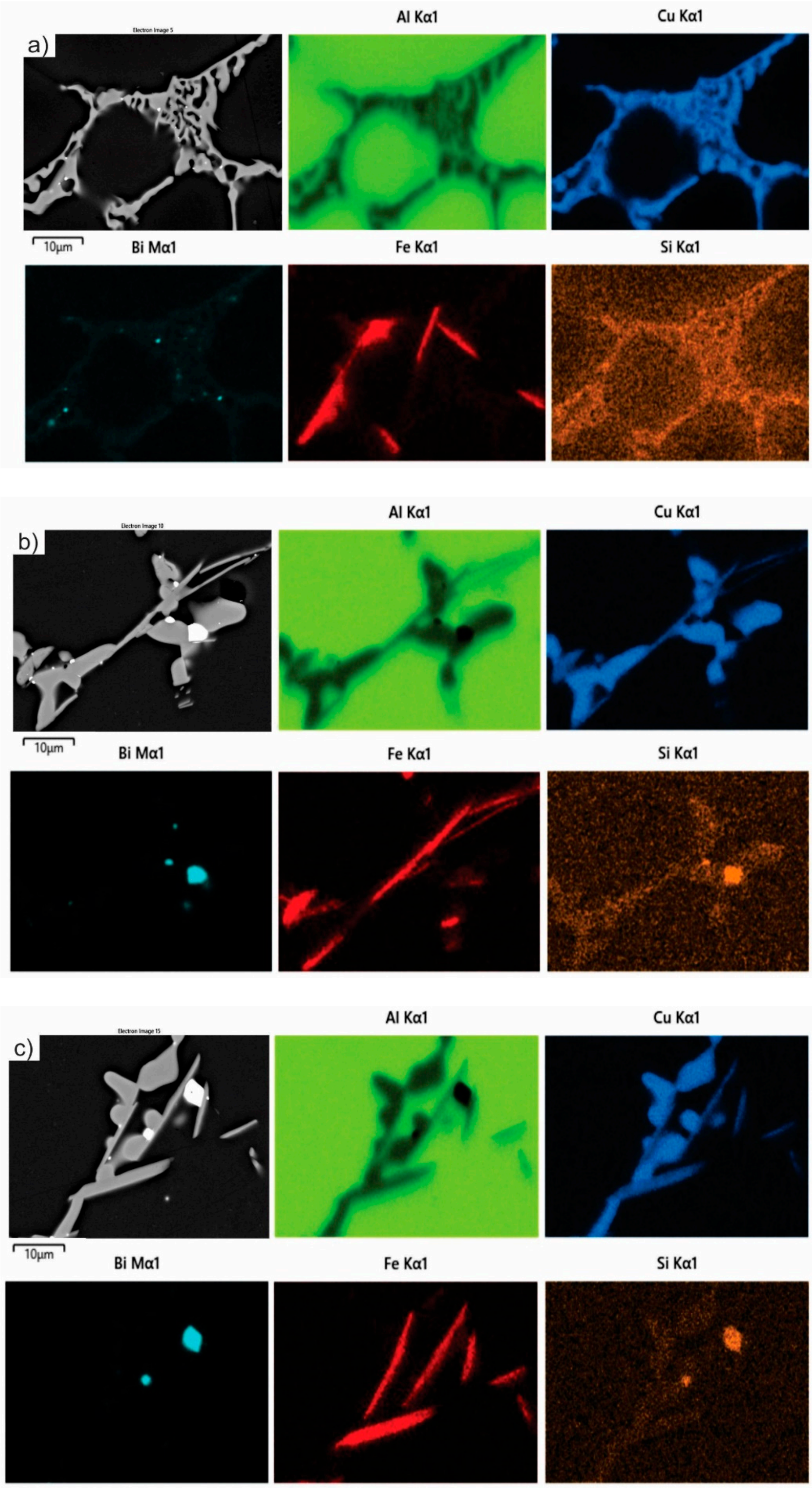

Figure 6. *Cont*.

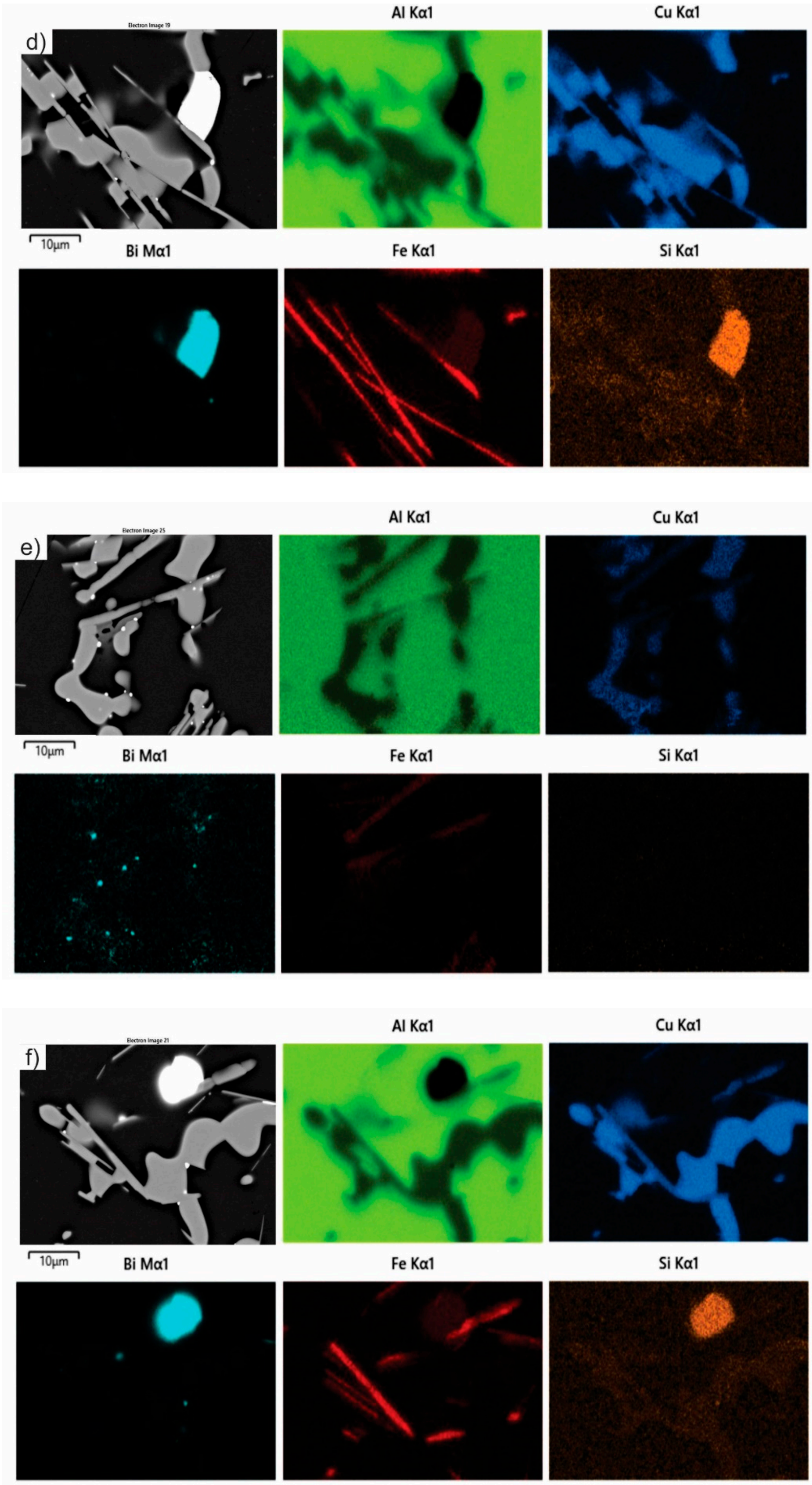

Figure 6. EDS individual elemental mapping analysis of as-cast (**a**) and homogenised samples at 520 °C for 4 h (**b**), 5 h (**c**), 6 h (**d**), 7 h (**e**), and 12 h (**f**) from modified EN AW 2011 aluminium alloy.

4. Conclusions

The homogenisation process of EN AW 2011 alloy allows for a more rounded shape of the Al_2Cu phase, equilibrium formation of the phases, and the precipitation in the matrix, leading to a rigorous increase in the hardness and is consistent with the hardness results. The alloy reaches optimal hardness after 4 h of homogenisation enabling still suitable extrudability. Further homogenisation time causes a further increase in hardness, subsequently causing a decrease in extrudability.

The experimental data revealed a suitable homogenisation time already after 4 h and not more than 6 h of homogenisation annealing at a temperature of 520 °C, enabling optimal extrusion properties. Longer homogenisation times at this temperature increases hardness of the alloys and makes modified EN AW 2011 aluminium alloy less extrudable.

Author Contributions: M.V. carried out the literature review, performed the experiments, analysed the results and wrote the paper; T.B. constructed the diagram and improved the idea for the paper; A.N. and I.P. made the measurements and carried out the metallography; B.Ž. made the hardness measurements and revised the paper; J.M. optimized the research program and revised the paper. All authors have read and agreed to the published version of the manuscript.

Funding: This research was funded by Republic of Slovenia, the Ministry of Education, Science and Sport, and the European Regional Development Fund. The work was carried out in the framework of the project "Modelling of Thermomechanical Processing of the Aluminium Alloys for High Quality Products: (MARTIN, Grant No.: OP20.03531). The authors would like to thank also to the Slovenian Research Agency (ARRS) for funding under program grant P2-0344.

Acknowledgments: The work was co-financed by the Republic of Slovenia, the Ministry of Education, Science and Sport, and the European Regional Development Fund. The work was carried out in the framework of the project "Modelling of Thermomechanical Processing of the Aluminium Alloys for High Quality Products: (MARTIN, Grant No.: OP20.03531). The authors would like to thank also to the Slovenian Research Agency (ARRS) for funding under program grant P2-0344.

Conflicts of Interest: The authors declare no conflict of interest.

References

1. Birol, Y. Age hardening of en AW 2014 alloy extruded in the semi-solid state. *Mater. Chem. Phys.* **2012**, *131*, 694–697. [CrossRef]
2. Zhou, W.; Lin, J.; Dean, T.A.; Wang, L. Analysis and modelling of a novel process for extruding curved metal alloy profiles. *Int. J. Mech. Sci.* **2018**, *138–139*, 524–536. [CrossRef]
3. Belov, N.A.; Eskin, D.G.; Avxentieva, N.N. Constituent phase diagrams of the Al-Cu-Fe-Mg-Ni-Si system and their application to the analysis of aluminium piston alloys. *Acta Mater.* **2005**, *53*, 4709–4722. [CrossRef]
4. Rinderer, B. The metallurgy of homogenization. *Mater. Sci. Forum* **2011**, *693*, 264–275. [CrossRef]
5. Sarafoglou, P.I.; Aristeidakis, J.S.; Tzini, M.I.T.; Haidemenopoulos, G.N. Metallographic index-based quantification of the homogenization state in extrudable aluminum alloys. *Metals* **2016**, *6*, 121. [CrossRef]
6. Gazizov, M.; Teleshov, V.; Zakharov, V.; Kaibyshev, R. Solidification behaviour and the effects of homogenisation on the structure of an Al-Cu-Mg-Ag-Sc alloy. *J. Alloys Compound.* **2011**, *509*, 9497–9507. [CrossRef]
7. Nadella, R.; Eskin, D.G.; Du, Q.; Katgerman, L. Macrosegregation in direct-chill casting of alumin-ium alloys. *Prog. Mater. Sci.* **2008**, *53*, 421–480. [CrossRef]
8. Ashiri, R.; Karimzadeh, F.; Niroumand, B. On effect of squeezing pressure on microstructural characteristics, heat treatment response and electrical conductivity of an Al-Si-Mg-Ni-Cu alloy. *Mater. Sci. Technol.* **2014**, *30*, 1162–1169. [CrossRef]
9. Kemsies, R.H.; Milkereit, B.; Wenner, S.; Holmestad, R.; Kessler, O. In situ DSC investigation into the kinetics and microstructure of dispersoid formation in Al-Mn-Fe-Si(-Mg) alloys. *Mater. Des.* **2018**, *146*, 96–107. [CrossRef]
10. Hatch, J.E. *Aluminum: Properties and Physical Metallurgy*; Hatch, J.E., Ed.; ASM International: Almere, The Netherlands, 1984.
11. Liu, C.L.; Azizi-Alizamini, H.; Parson, N.C.; Poole, W.J.; Du, Q. Microstructure evolution during homogenization of Al-Mg-Si-Mn-Fe alloys: Modelling and experimental results. *Trans. Nonferr. Met. Soc. China* **2017**, *27*, 747–753. [CrossRef]
12. Vončina, M.; Kresnik, K.; Volšak, D.; Medved, J. Effects of homogenization conditions on the microstructure evolution of aluminium alloy EN AW 8006. *Metals* **2020**, *10*, 419. [CrossRef]
13. Wang, S.C.; Starink, M.J. Precipitates and intermetallic phases in precipitation hardening Al-Cu-Mg-(Li) based alloys. *Int. Mater. Rev.* **2005**, *50*, 193–215. [CrossRef]
14. McKeown, J.T.; Kulovits, A.K.; Liu, C.; Zweiacker, K.; Reed, B.W.; Lagrange, T.; Wiezorek, J.M.K.; Campbell, G.H. In situ transmission electron microscopy of crystal growth-mode transitions during rapid solidification of a hypoeutectic Al-Cu alloy. *Acta Mater.* **2014**, *65*, 56–68. [CrossRef]

15. Li, C.; Sha, G.; Gun, B.; Xia, J.H.; Liu, X.F.; Wu, Y.Y.; Birbilis, N.; Ringer, S.P. Enhanced age-hardening response of Al-4Mg-1Cu (wt.%) microalloyed with Ag and Si. *Scr. Mater.* **2013**, *68*, 857–860. [CrossRef]
16. Gazizov, M.R.; Dubina, A.V.; Zhemchuzhnikova, D.A.; Kaibyshev, R.O. Effect of equal-channel angular pressing and aging on the microstructure and mechanical properties of an Al-Cu-Mg-Si al-loy. *Phys. Met. Metallogr.* **2015**, *116*, 718–729. [CrossRef]
17. Joshi, A.; Yogesha, K.K.; Kumar, N.; Jayaganthan, R. Influence of Annealing on Microstructural Evolution, Precipitation Sequence, and Fracture Toughness of Cryorolled Al–Cu–Si Alloy. *Metallogr. Microstruct. Anal.* **2016**, *5*, 540–556. [CrossRef]
18. Ghosh, K.S.; Tripati, K. Microstructural characterization and electrochemical behavior of AA2014 Al-Cu-Mg-Si alloy of various tempers. *J. Mater. Eng. Perform.* **2018**, *27*, 5926–5937. [CrossRef]
19. Mirkovicá, D.; Gröbner, J.; Kaban, I.; Hoyer, W.; Schmid-Fetzer, R. Integrated approach to thermo-dynamics, phase relations, liquid densities and solidification microstructures in the Al-Bi-Cu system. *Int. J. Mater. Res.* **2009**, *100*, 176–188. [CrossRef]
20. Shi, Y.J.; Pan, Q.L.; Li, M.J.; Liu, Z.M.; Huang, Z.Q. Microstructural evolution during homogenization of DC cast 7085 aluminum alloy. *Trans. Nonferr. Met. Soc. China* **2015**, *25*, 3560–3568. [CrossRef]
21. Standardization, E.C.F. European Standard 2007. Available online: https://metcenter.ru/f/en_573-3.pdf (accessed on 11 November 2020).
22. Shaha, S.K.; Czerwinski, F.; Kasprzak, W.; Friedman, J.; Chen, D.L. Thermal stability of (AlSi)×(ZrVTi) intermetallic phases in the Al–Si–Cu–Mg cast alloy with additions of Ti, V and Zr. *Thermochim. Acta* **2014**, *595*, 11–16. [CrossRef]
23. Jo, H.H.; Cho, H.; Lee, K.W.; Kim, Y.J. Extrudability improvement and energy consumption estimation in Al extrusion process of a 7003 alloy. *J. Mater. Process. Technol.* **2002**, *130–131*, 407–410. [CrossRef]
24. Lee, S.K.; Ko, D.C.; Kim, B.M. Optimal die profile design for uniform microstructure in hot extruded product. *Int. J. Mach. Tools Manuf.* **2000**, *40*, 1457–1478. [CrossRef]
25. Vončina, M.; Paulin, I.; Debevec, A.; Nagode, A. Modification of the cast structure of an EN AW 2011 alloy with homogenization. *Mater. Technol.* **2021**, *55*, 2. [CrossRef]
26. Porter, D.A.; Easterling, K.E.; Sherif, M.Y. *Phase Transformations in Metals and Alloys*, 3rd ed.; Porter, D.A., Easterling, K.E., Sherif, M.Y., Eds.; CRC Press: Boca Raton, FL, USA, 2009; ISBN 9781420062106.